The extended depletion model presented above allows for estimation of the extent of the depletion effect attributable to stone growth itself and takes into account the individual variability of the differential volume function of a patient's kidneys. Moreover, it confirms that the usual practice of neglecting variation in the differential function within normal values ($0.44 \leq \gamma \leq 0.56$) is appropriate in the context of stone formation.

References

1. Laube N, Pullmann M, Hergarten S, Hesse A. Influence of urinary stones on the composition of a 24-hour urine sample. Clin Chem 2003;49:281–5.
2. Laube N, Pullmann M, Hergarten S, Schmidt M, Hesse A. The alteration of urine composition due to stone material present in the urinary tract. Eur Urol 2003;44:595–9.
3. Hesse A, Brändle E, Wilbert D, Köhrmann KU, Alken P. Study on the prevalence and incidence of urolithiasis in Germany comparing the years 1979 vs. 2000. Eur Urol 2003;44:709–13.
4. Kavanagh JP. Enlargement of a lower pole calcium oxalate stone: a theoretical examination of the role of crystal nucleation, growth, and aggregation. J Endurol 1999;13:605–10.
5. Sutton RAL, Walker VR. Enteric and metabolic hyperoxaluria. Miner Electrolyte Metab 1994;20:352–60.
6. Robertson WG, Hughes H. Importance of mild hyperoxaluria in the pathogenesis of urolithiasis—new evidence from studies in the Arabian Peninsula. Scan Microsc 1993;7:391–402.

DOI: 10.1373/clinchem.2004.035972

Comparison of Reverse Transcriptases in Gene Expression Analysis, *Anders Ståhlberg,[1,2*] Mikael Kubista,[1,2] and Michael Pfaffl[3]* ([1]Department of Chemistry and Biosciences, Chalmers University of Technology, Gothenburg, Sweden; [2]TATAA Biocenter, Gothenburg, Sweden; [3]Physiology Weihenstephan, Center of Life and Food Sciences, Technical University of Munich, Munich, Germany; * address correspondence to this author at: Department of Chemistry and Biosciences, Chalmers University of Technology, Medicinaregatan 7B, 405 30 Gothenburg, Sweden; fax 46317733910, e-mail anders.stalberg@tataa.com)

In most measurements of gene expression, mRNA is first reverse-transcribed into cDNA. The reverse transcription reaction is not very well understood, and it is expected to be the uncertain step in gene expression analysis. It can introduce errors produced by effects of mRNA secondary and tertiary structures, variation in priming efficiency, and properties of the reverse transcriptase *(1–5)*. The aim of this work was to study the yield, reproducibility, and sensitivity of some commercially available reverse transcriptases on low to intermediate expressed genes by use of quantitative real-time PCR (QPCR).

Total RNA extraction, reverse transcription, and QPCR were performed as described in the Data Supplement that accompanies the online version of this Technical Brief at http://www.clinchem.org/content/vol50/issue9/ *(6, 7)*. All reverse transcription reactions were run in replicates of four, using starting material from the same RNA pool prepared from bovine spleen, liver, or jejunum, which eliminated sample-to-sample variation *(8)*. Only results for RNA from spleen are shown. Liver and jejunum gave similar results, which are provided in the online Data Supplement. To determine absolute reverse transcription yields, we added an artificial RNA MultiStandard (Roboscreen) to samples *(9, 10)*. Eight reverse transcriptases were studied: Moloney murine leukemia virus RNase H^- (MMLVH; Promega); MMLV (Promega); avian myeloblastosis virus (AMV; Promega); Improm-II (Promega); Omniscript (Qiagen); cloned AMV (cAMV; Invitrogen); ThermoScript RNase H^- (Invitrogen); and SuperScript III RNase H^- (Invitrogen). Reverse transcription with AMV, MMLV, and Omniscript was performed at 37 °C, whereas with cAMV, Improm-II, and MMLVH it was performed at 45 °C, and with ThermoScript and SuperScript, it was performed at 50 °C.

The cDNA synthesis yields of the intermediate to highly expressed β-actin and glyceraldehyde-3-phosphate dehydrogenase (GAPDH) genes and the low expressed genes 5-hydroxytryptamine 1a receptor (HTR1a), HTR1b, HTR2a, and HTR2b were measured by QPCR using SYBR Green I detection chemistry *(7)*. The mean threshold cycle (Ct) and corresponding SD for all combinations of genes and reverse transcriptases are shown in Fig. 1. Because of the exponential behavior of PCR, a difference of 1 cycle in Ct between runs that differed only in the reverse transcriptase used corresponded to twofold difference in reverse transcription yield (assuming 100% PCR efficiency). For HTR1a, HTR1b, and HTR2b, the reverse transcription yields obtained with the eight reverse transcriptases were similar, whereas for GAPDH and, in particular, for HTR2a and β-actin, substantial variations were observed (Fig. 1). For example, for HTR2a, the Ct was 32.3 cycles when SuperScript III was used, whereas it was 38.8 cycles when AMV was used. This corresponds to a $2^{6.5} = 91$-fold difference in reverse transcription yield. For HTR2b, the difference in yield with the two enzymes was only $2^{25.4 - 25.2} = 1.14$, which is 14%.

Primer hybridization relies on access to the appropriate target site in the mRNA and may vary substantially because of mRNA folding *(11, 12)*. Reverse transcription yields could vary among the reverse transcriptases in a highly gene-dependent way as a consequence of mRNA secondary and tertiary structures. Large variation is expected for mRNAs with tight structures in which access to primer target sites is restricted. Our data suggest that this may be the case for β-actin, GAPDH, and HTR2 with our choice of primers. The reverse transcriptase that performed best for these genes was SuperScript III, which was used at 50 °C. A higher annealing temperature is often claimed to improve reverse transcription yields by reducing the degree of mRNA secondary structure, but ThermoScript, which also was used at 50 °C, did not perform particularly well. Furthermore, we found no advantage when we used reverse transcriptases without RNase activity (MMLVH, SuperScript III, and ThermoScript), which also is claimed by some vendors to improve transcription efficiency. For the six genes studied, SuperScript III gave the overall highest yield, followed by

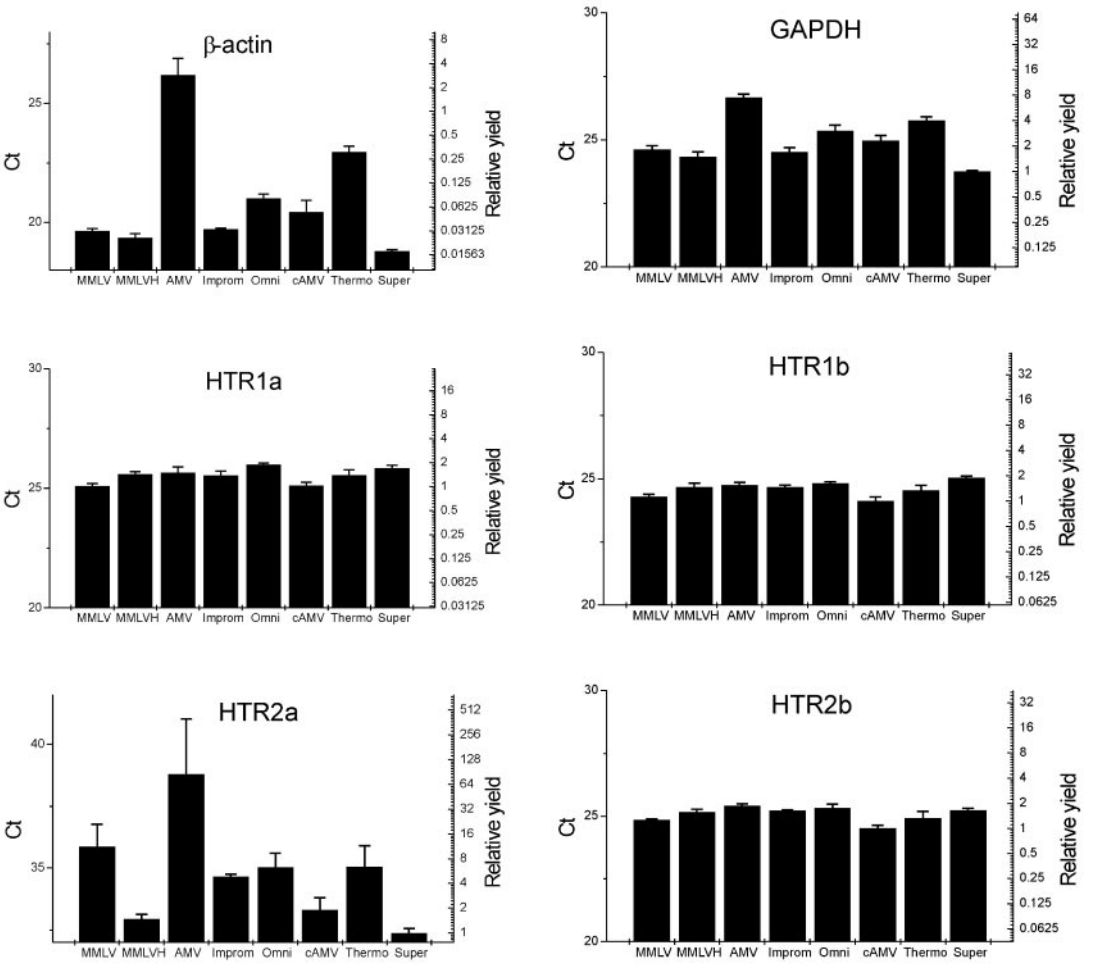

Fig. 1. QPCR Ct values reflecting the amounts of cDNA produced by the reverse transcriptases, with total RNA from spleen as input material.

Error bars indicate SD of samples run in quadruplicate. Yields relative to the least efficient reverse transcriptase, expressed in number of cDNA copies (assuming 100% PCR efficiency), are indicated by the *right-hand y axis*. The reverse transcriptases are as follows: (*left* to *right*) MMLV, MMLVH, AMV, Improm-II (*Improm*); Omniscript (*Omni*), cAMV, ThermoScript (*Thermo*), and SuperScript III (*Super*).

MMLVH and cAMV. AMV gave the poorest yield. The reproducibility, represented as SD of repeated experiments (Fig. 1), was very high with all reverse transcriptases for all genes studied but HTR2a. This could be attributable to statistical variation at low copy numbers for HTR2a, which is expressed at very low yield *(13)*.

For absolute determination of reverse transcription yields, the systems were calibrated by addition of RNA/DNA MultiStandard molecules (Roboscreen) of known concentrations. The reverse transcription yield is defined as:

$$\text{Yield (\%)} = \frac{n_{cDNA}}{n_{mRNA}} \times 100 \quad (1)$$

n_{mRNA} is the number of mRNA molecules of a particular gene in the test sample, and n_{cDNA} is the number of cDNA copies for that mRNA that are produced by reverse transcription. From the calibration curve of the DNA MultiStandard (10–10^6 DNA molecules), we obtain *(14)*:

$$Ct = 38.34 - 3.49 \times \log(n_{cDNA}) \quad (2)$$

The slope (−3.49) reflects a PCR efficiency of 93%. When we instead added RNA MultiStandard with the same sequence as the DNA standard to the test samples and reverse transcribed it before QPCR, the reverse transcription yield could be calculated as:

$$\text{Yield (\%)} = \frac{10^{-\left(\frac{Ct - 38.34}{3.49}\right)}}{n_{mRNA}} \times 100 \quad (3)$$

When we added 10^4–10^6 RNA molecules, we obtained similar reverse transcription yields, whereas with 10^3 RNA molecules, the yields were substantially higher (Table 1). This is probably an artifact attributable to too few RNA molecules (diluted 1:29) in the final running solution and formation of primer-dimer products detected by SYBR Green I chemistry. The latter may be avoided by use of specific probes. These data were therefore not considered when we calculated mean yields.

The detection of rare mRNA transcripts is often an issue. The yield of low-abundance mRNA has been

Table 1. Absolute reverse transcription yields for RNA.

	Mean (SD) yields[a] (%) at external RNA input (in molecules) of:				Mean (SD)[b] yield for RNA MultiStandard, %
	10^6	10^5	10^4	10^3	
MMLVH	22	50	48	125	40 (16)
Omniscript	7.2	3.1	11.5	66	7.3 (4.2)
AMV	0.4	0.6	4.9	44	2.0 (2.5)
MMLV	32	49	50	110	44 (10)
Improm-II	32	22	12	98	22 (10)
cAMV	6.3	17	35	88	19 (15)
ThermoScript	1.1	9.0	14	46	8.0 (6.6)
SuperScript III	87	72	90	43	83 (10)
Mean (SD)	24 (29)	28 (26)	33 (29)	78 (32)	28 (27)

[a] Reverse transcription yields of RNA prepared from liver and spleen. The samples were diluted 30-fold before QPCR measurements, giving initial copy numbers of 33–33 333 molecules/sample. Note the markedly higher yields at an input of 10^3 RNA molecules.

[b] Reverse transcription yield for samples containing 10^4-10^6 RNA MultiStandard molecules.

shown to be significantly improved when carrier is used *(1, 15)*. The reverse transcription yields for the RNA MultiStandard varied more than 100-fold. The lowest yield (0.4%) was obtained with AMV for 10^6 RNA molecules, and the highest yield (90%) was obtained with SuperScript III for 10^4 RNA molecules (Table 1). The latter was overall the most efficient reverse transcriptase, with a mean yield of 83%. MMLV and MMLVH gave mean yields of 44% and 40%, respectively, whereas the mean yields of the other reverse transcriptases were <25%. The yield obtained with MMLVH was comparable to that reported in a previous study *(15)*.

In conclusion, we show that reverse transcription yields vary up to 100-fold with the choice of reverse transcriptase and that the variation is gene dependent. Previously, we also reported a dependence on priming strategy *(1)*. Hence, for quantitative gene expression measurements based on reverse transcription to be comparable among laboratories, the same enzyme, priming strategy, and experimental conditions must be used.

This work was supported by Deutsche Forschungsgemeinschaft, the Chalmers Bioscience effort, and the Crafoord Foundation.

References

1. Ståhlberg A, Håkansson J, Xian X, Semb H, Kubista M. Properties of the reverse transcription reaction in mRNA quantification. Clin Chem 2004;50:509–15.
2. Polumuri SK, Ruknudin A, Schulze DH. RNase H and its effects on PCR. Biotechniques 2002;32:1224–5.
3. Mayers TW, Gelfand DH. Reverse transcription and DNA amplification by *Thermus thermophilus* DNA polymerase. Biochem 1991;30:7661–6.
4. Brooks EM, Sheflin LG, Spaulding SW. Secondary structure in the 3′UTR of EGF and the choice of reverse transcriptases affect the detection of message diversity by RT-PCR. Biotechniques 1995;19:806–15.
5. Kuo KW, Leung M, Leung WC. Intrinsic secondary structure of human TNFR-I mRNA influences the determination of gene expression by RT-PCR. Mol Cell Biochem 1997;177:1–6.
6. Pfaffl MW, Hageleit M. Validities of mRNA quantification using recombinant RNA and recombinant DNA external calibration curves in real-time RT-PCR. Biotechnol Letters 2001;23:275–82.
7. Reist M, Pfaffl MW, Morel C, Meylan M, Hirsbrunner G, Blum JW, et al. Quantitative mRNA analysis of bovine 5-HT receptor subtypes in brain, abomasums, and intestine by real-time PCR. J Recept Signal Transduct Res 2003;23:271–87.
8. Ståhlberg A, Åman P, Ridell B, Mostad P, Kubista M. Quantitative real-time PCR method for detection of B-lymphocyte monoclonality by comparison of κ and λ immunoglobulin light chain expression. Clin Chem 2003;49:51–9.
9. Köhler T. Design of suitable primers and competitor fragments for quantitative PCR. In: Köhler T, Lassner D, Rost AK, Thamm B, Pustowoit B, Remke H, eds. Quantitation of mRNA by polymerase chain reaction—nonradioactive PCR methods. Heidelberg: Springer-Verlag, 1995;1.2:15–26.
10. Köhler T, Lerche D, Meye A, Weisbrich C, Wagner O. Automated analysis of nucleic acids by quantitative PCR using DNA coated ready-to-use reaction tubes. J Lab Med 1999;23:408–14.
11. Southern EM, Kalim UM. Determining the influence of structure on hybridization using oligonucleotide arrays. Nat Biotechnol 1999;17:788–92.
12. Sohail M, Southern EM. Hybridization of antisense reagents to RNA. Curr Opin Mol Ther 2000;2:264–71.
13. Peccoud J, Jacob C. Theoretical uncertainty of measurements using quantitative polymerase chain reaction. Biophys J 1996;71:1001–8.
14. Pfaffl MW. A new mathematical model for relative quantification in real-time RT-PCR. Nucleic Acids Res 2001;29:e45.
15. Curry J, McHale C, Smith MT. Low efficiency of the Moloney murine leukemia virus reverse transcriptase during reverse transcription of rare t(8;21) fusion gene transcripts. Biotechniques 2002;32:768–75.

DOI: 10.1373/clinchem.2004.035469

Multiplexed Real-Time PCR Using Universal Reporters,

*Andreas M. Rickert, Hans Lehrach, and Silke Sperling** (Max-Planck-Institute for Molecular Genetics, Berlin, Germany; * address correspondence to this author at: Max-Planck-Institute for Molecular Genetics, Ihnestrasse 73, 14195 Berlin, Germany; fax 49-30-8413-1128, e-mail sperling @molgen.mpg.de)

Real-time quantitative PCR is a sensitive and accurate method for gene expression studies *(1)*. The detection chemistries of all real-time PCR procedures are based on one of two principles for monitoring amplification products: binding to double-stranded DNA or hybridization to single-stranded DNA. Small molecules bind to double-stranded DNA either as intercalators or as minor groove binders, e.g., ethidium bromide *(2)*, Hoechst 33258 *(3)*, or SYBR® Green I *(4)*. Several approaches using target-specific hybridization to single-stranded DNA have been introduced, including Molecular Beacons *(5)*, Scorpions *(6, 7)*, the TaqMan or hydrolysis/5′-nuclease assay *(8, 9)*, the AEGIS probe system *(10)*, labeled primers *(11, 12)*, and light-up probes *(13)*. In contrast to binding of dyes to double-stranded DNA, these methods are suitable for multiplexing approaches because they use differentially labeled fluorescent dyes. However, as they require a unique probe or modified primer for each target, currently used hybridization-based methods for real-time quantitative PCR have high reagent costs and require large developmental efforts.

Here we present a real-time PCR assay that uses universal hybridization-based probe sets suitable for any target. Because the assay uses tailed locus-specific non-modified amplification primers, PCR products can be

Data Supplement

Materials and Methods

RNA isolation and reverse transcription

Total RNA extraction was performed from bovine liver, spleen and jejunum, using *TriFast* (Peqlab, Erlangen, Germany) as described by manufacturers' instructions. Eight syntheses were performed using the reverse transcriptases according to manufacturers' instructions. Same concentration of random hexamers (5 μM), dNTP (500μM) and RNase inhibitor (25U) were used in all reactions. Reaction volume was 7 μL and experimental protocol was: 300 ng total RNA, random hexamers, and RNA MultiStandard (10^6, 10^5, 10^4 and 10^3 RNA molecules, Roboscreen, Leipzig, Germany) (9-10) was denaturated at 70 ˚C for 5 min and then chilled on ice before adding the remaining components. The samples were first incubated at 25 ˚C for 10 min and then for 50 min either at 37 ˚C for AMV, MMLV, and Omniscript, or at 45 ˚C for MMLVH, Improm-II, and cAMV, or at 50 ˚C for ThermoScript and SuperScript III. Finally the reaction was terminated by heating to 93 ˚C for 3 min.

Real-time PCR

Each real-time PCR master-mix contained 6.4 μL water, 1.2 μL $MgCl_2$ (4 mM), 0.2 μL of each primer (0.4 μM), 1.0 μL LightCycler Fast Start DNA Master SYBR Green I mix (Roche Diagnostics, Mannheim, Germany), and 1 μL (10 ng) reverse transcribed total RNA. Real-time PCR was performed in a LightCycler (Roche Diagnostics) starting with 10 min preincubation at 95 ˚C followed by 50 amplification cycles, as described earlier (7). Denaturation was performed at 95 ˚C for 15 sec, and annealing, elongation, and acquisition as specified in Supplemental Data Table 1. Ct was determined using the maximum second derivate function in the LightCycler software (Roche Diagnostics). Formation of expected PCR product was confirmed by agarose gel electrophoresis (2 % w/v) and melting curve

analysis. For absolute quantification RNA and DNA MultiStandard molecules (Roboscreen) of known concentrations were used. Samples were spiked with 10^3 - 10^6 RNA standard molecules, and diluted 30 times before QPCR analysis. Final amounts of RNA standard was to 33-33,333 molecules per capillary reaction setup.

Figure Legends

Supplemental Data Figure 1. QPCR Ct values reflecting the amounts of cDNAs produced by the reverse transcriptases, using total RNA from jejunum. Reverse transcription with AMV of the HTR2a gene gave no yield (star). Yields relative to the least efficient reverse transcriptase, expressed in number of cDNA copies (assuming 100 % PCR efficiency), are indicated by the right-hand y axis.

Supplemental Data Figure 2. QPCR Ct values reflecting the amounts of cDNAs produced by the reverse transcriptases, using total RNA from liver. Reverse transcription of the HTR2a gene gave no yield for some reverse transcriptases (star). Yields relative to the least efficient reverse transcriptase, expressed in number of cDNA copies (assuming 100 % PCR efficiency), are indicated by the right-hand y axis.

Table

Supplemental Data Table 1. Real-time PCR assays

Gene	Primer sequence	Anneling	Elongation	Acquisition	Acc. No.
B-actin	5'-AACTCCATCATGAAGTGTGACG-3'	60˚C (10sec)	72˚C (20sec)	88˚C(5sec)	AY141970
	5'-GATGGACATCTGCTGGAAGG-3'				
GAPDH	5'-GTCTTCACTACCATGGAGAAGG-3'	58˚C (10sec)	72˚C (20sec)	86˚C (5sec)	BTU85042
	5'-TCATGGATGACCTTGGCCAG-3'				
HTR1a	5'-TCAGCTACCAAGTGATCACCTCT-3'	60˚C (10sec)	72˚C (25sec)	88˚C (5sec)	AJ491858
	5'-GTCCACTTGTTGAGCACCTG-3'				
HTR1b	5'-TGCTCCTCATCGCCCTCTATG-3'	60˚C (10sec)	72˚C (25sec)	86˚C (5sec)	AJ491859
	5'-CTAGCGGCCATGAGTTTCTTCTT-3'				
HTR2a	5'-AGCTGCAGAATGCCACCAACTAT-3'	60˚C (10sec)	72˚C (25sec)	86˚C (5sec)	AJ491863
	5'-GGTATTGGCATGGATATACCTAC-3'				
HTR2b	5'-AAACAAGCCACCTCAACGCCT-3'	60˚C (10sec)	72˚C (25sec)	81˚C (5sec)	AJ291864
	5'-TCCCGAAATGTCTTATTGAAGAG-3'				
MultiStandard[a]		59˚C (10sec)	72˚C (20sec)	78˚C (5sec)	

[a]Primer sequences for the MultiStandard are not available

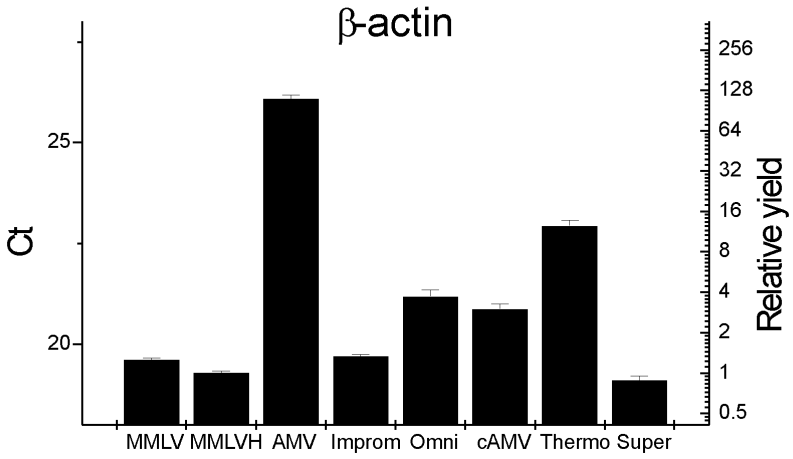
β-actin
Ct
Relative yield
25
20
256
128
64
32
16
8
4
2
1
0.5
MMLV MMLVH AMV Improm Omni cAMV Thermo Super

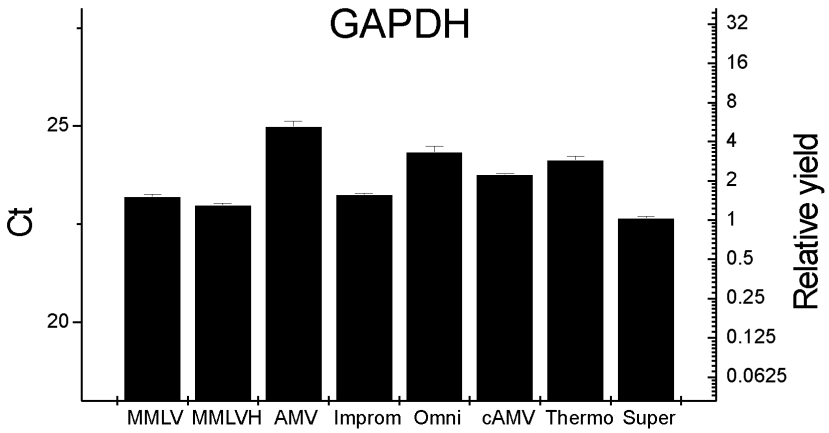
GAPDH
Ct
Relative yield
25
20
32
16
8
4
2
1
0.5
0.25
0.125
0.0625
MMLV MMLVH AMV Improm Omni cAMV Thermo Super

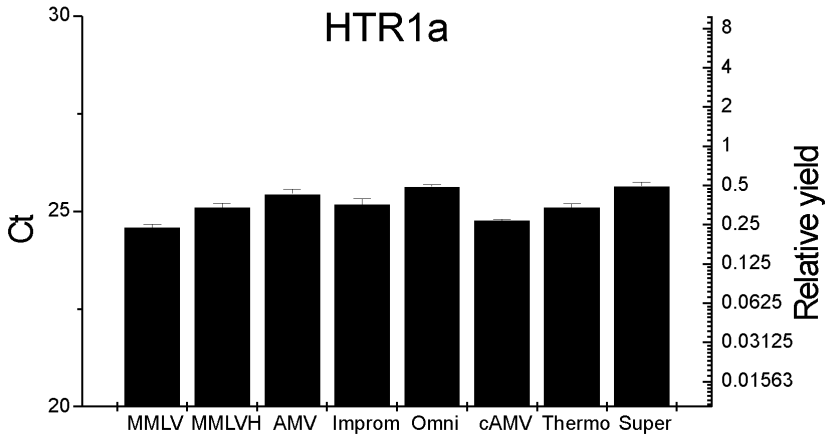
HTR1a
Ct
Relative yield
30
25
20
8
4
2
1
0.5
0.25
0.125
0.0625
0.03125
0.01563
MMLV MMLVH AMV Improm Omni cAMV Thermo Super

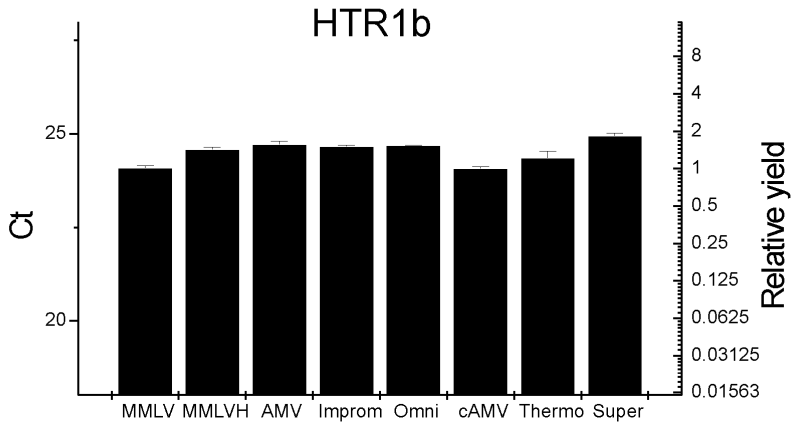
HTR1b
Ct
Relative yield
25
20
8
4
2
1
0.5
0.25
0.125
0.0625
0.03125
0.01563
MMLV MMLVH AMV Improm Omni cAMV Thermo Super

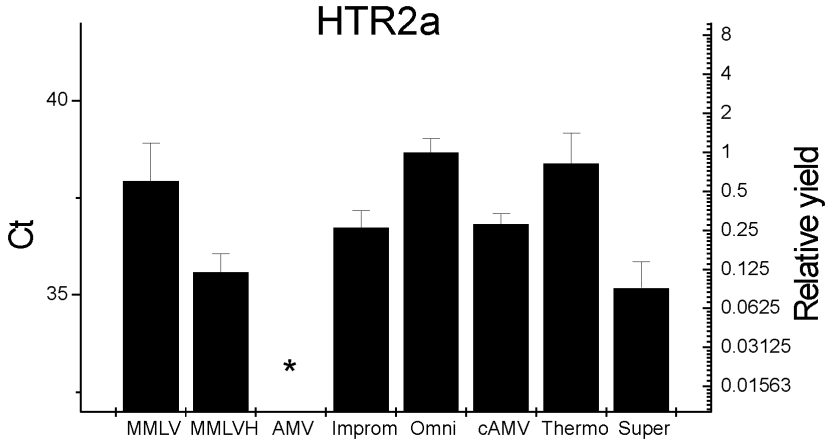
HTR2a
Ct
Relative yield
40
35
*
8
4
2
1
0.5
0.25
0.125
0.0625
0.03125
0.01563
MMLV MMLVH AMV Improm Omni cAMV Thermo Super

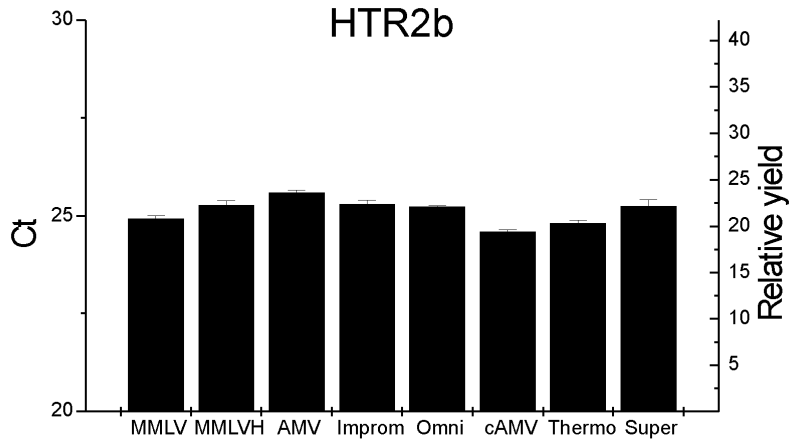
HTR2b
Ct
Relative yield
30
25
20
40
35
30
25
20
15
10
5
MMLV MMLVH AMV Improm Omni cAMV Thermo Super

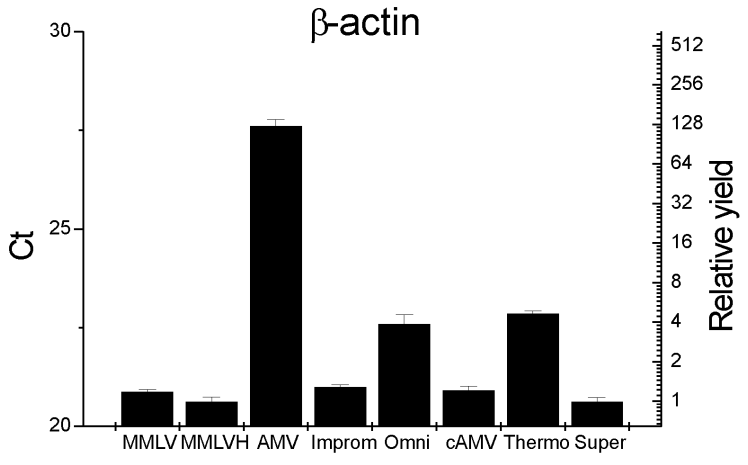
β-actin
Ct
Relative yield
30
25
20
512
256
128
64
32
16
8
4
2
1
MMLV MMLVH AMV Improm Omni cAMV Thermo Super

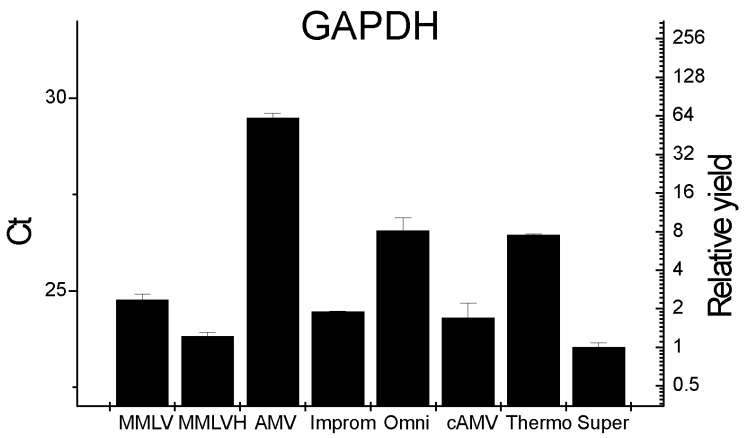
GAPDH
Ct
Relative yield
30
25
256
128
64
32
16
8
4
2
1
0.5
MMLV MMLVH AMV Improm Omni cAMV Thermo Super

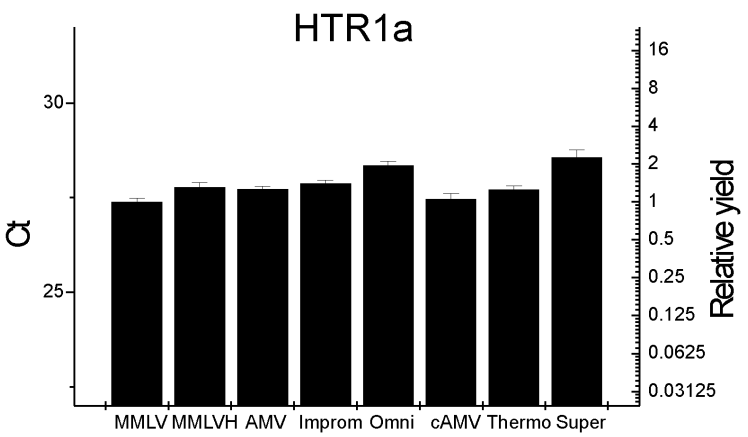
HTR1a
Ct
Relative yield
30
25
16
8
4
2
1
0.5
0.25
0.125
0.0625
0.03125
MMLV MMLVH AMV Improm Omni cAMV Thermo Super

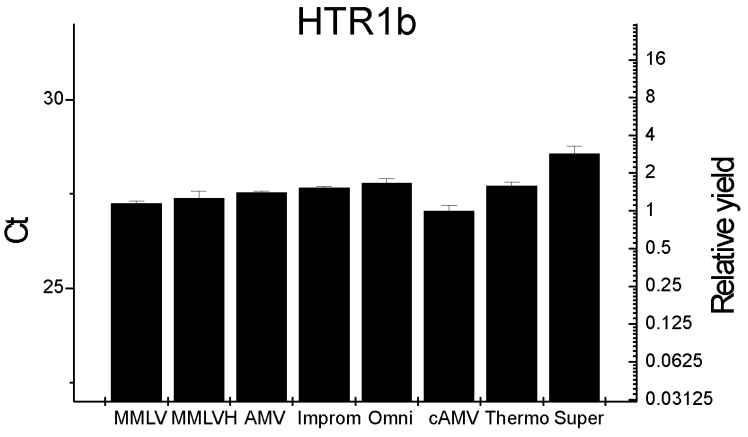
HTR1b
Ct
Relative yield
30
25
16
8
4
2
1
0.5
0.25
0.125
0.0625
0.03125
MMLV MMLVH AMV Improm Omni cAMV Thermo Super

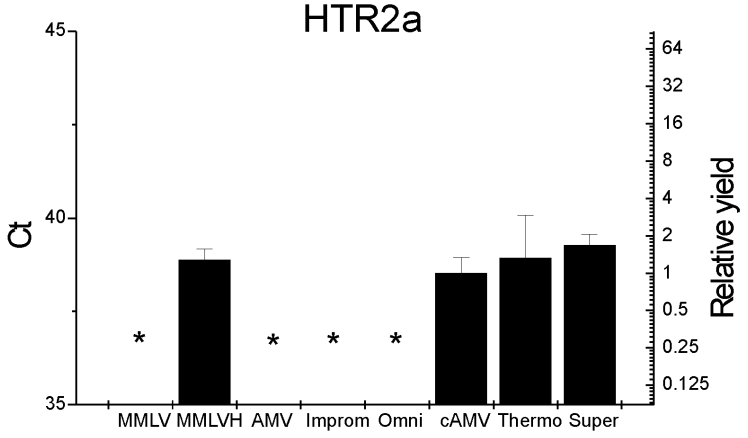
HTR2a
Ct
Relative yield
45
40
35
64
32
16
8
4
2
1
0.5
0.25
0.125
*
*
*
*
MMLV MMLVH AMV Improm Omni cAMV Thermo Super

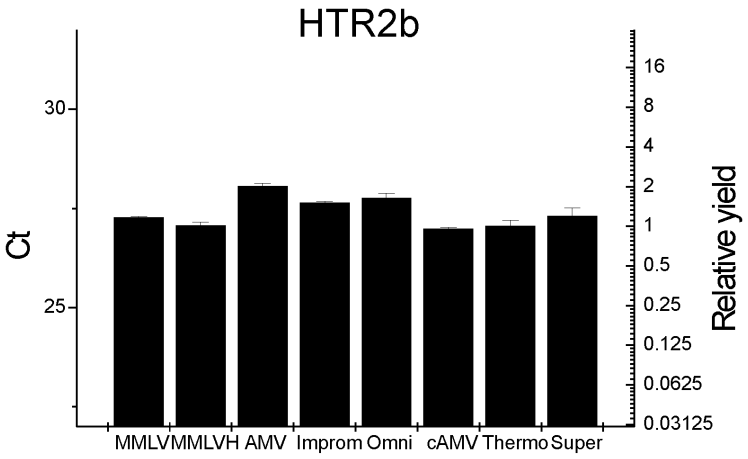
HTR2b
Ct
Relative yield
30
25
16
8
4
2
1
0.5
0.25
0.125
0.0625
0.03125
MMLV MMLVH AMV Improm Omni cAMV Thermo Super